Design of Ultra-High Performance Concrete Jetty in Marine Environment

Conference Paper · August 2014

CITATION
1

READS
338

5 authors, including:

Yen Lei Voo
DURA Technology Sdn Bhd
23 PUBLICATIONS **330** CITATIONS
SEE PROFILE

Sukhvinder Singh
PEC University of Technology
1 PUBLICATION **1** CITATION
SEE PROFILE

Design of Ultra-High Performance Concrete Jetty in Marine Environment

Yen Lei, VOO[1], Kuna Sittampalam[2], Chen Wai Peng[3], Sukhvinder Singh[4]

[1] CEO & Director, Dura Technology Sdn Bhd, Lot 304993, Jalan Chepor 11/8, Pusat Seramik Fasa 2, Ulu Chepor, 31200, Chemor, Perak, Malaysia. Email: vooyenlei@dura.com.my
Adjunct Professor, Civil Engineering Department, Universiti Putra Malaysia (UPM), Serdang, Malaysia.

[2] Executive Director, HSS Integrated Sdn Bhd, B-1 (1-4) Block B, Plaza Dwitasik, No. 21, Jalan 5/106, Bandar Sri Permaisuri, 56000, Kuala Lumpur, Malaysia. Email: kuna@hss.com.my

[3] Consultant, HSS Integrated Sdn Bhd, B-1 (1-4) Block B, Plaza Dwitasik, No. 21, Jalan 5/106, Bandar Sri Permaisuri, 56000, Kuala Lumpur, Malaysia. Email: wpchen@hss.com.my

[4] Bridge/Port Engineer, HSS Integrated Sdn Bhd, B-1 (1-4) Block B, Plaza Dwitasik, No. 21, Jalan 5/106, Bandar Sri Permaisuri, 56000, Kuala Lumpur, Malaysia. Email: sukhvinder@hss.com.my

ABSTRACT

This paper highlights some of the major design aspects of Malaysia's first multi-span composite bridge in marine environment constructed using the technology of ultra-high performance concrete (UHPC). Sustainability design approach (SDA) was used in the bridge design and the model mainly consists of three aspects, namely: (i) environmental impact assessment, (ii) durability design and (iii) limit state design. Examples on the environmental impact assessment (EIA) of the UHPC composite bridge compared to that of conventional reinforced concrete design are presented herein and the comparison studies show that the UHPC composite bridge generally is more eco-friendly than the conventional RC bridge in terms of reduction of raw material consumption, CO_2 emissions, embodied energy and global warming potential. Besides that, example on durability design (DD) shows the enhanced durability of UHPC also provides for significant improvements in the structure's service life or design life, which further supports the concept of sustainable development. Lastly, performance load proof test on the full-scale bridge girders were tested, and the test results show the precast UHPC girders generally can meet the design requirements.

Keywords: Ultra-high performance concrete, marine, jetty, fiber.

1 INTRODUCTION

Ultra-high performance concrete (UHPC) is an advanced cementitious-based composite material that offers new opportunities for current or future infrastructure development in both urban-suburban regions and rural developments. UHPC in its present form has become commercially available in many countries such as Australia, Austria, Canada, Germany, Italy, Japan, Malaysia, Netherlands, New Zealand, Slovenia, South Korea, the United States and other countries. A complete search of the literature has identified more than 100 completed bridges (pedestrian and motorway bridges combined) constructed using UHPC in one or more components. Both private and governmental bodies are directing attention and initiative towards exploiting UHPC as the future construction material, in the belief that UHPC technology embraces the complete solution for sustainable constructions or sustainable development (Voo & Foster, 2010).

In 2012, Westports Malaysia Sdn. Bhd. called tenders to expand their container cargo terminal at Pulau Indah, Port Klang. The project included the construction of four new access bridges (namely Bridge24, Bridge25, Bridge26 and Bridge27) connecting the new wharf to the container stacking yard. One of the four bridges, Bridge25, was to be designed as a special access bridge for overweight and oversized cargo with trailer payloads up to 3,000 metric tonnes. The project owner, Westports Malaysia Sdn. Bhd. had engaged HSS Integrated Sdn. Bhd. (HSSI) as the Engineer for the project and Putra Perdana Construction Sdn. Bhd. as the Contractor. HSSI specified the use of Grade150 UHPC precast prestressed beams for Bridge25 in order to carry the exceptionally heavy live loads while maintaining a shallow beam depth of 1m. The material has also been reported to be highly durable and had the ability to provide a service life in excess of 100 years (JSCE, 2006). Being located in the marine environment, Bridge25 would benefit from UHPC's extra resistance against chloride attack, which would be a major advantage. The other three bridges adopted conventional Grade50 concrete composite bridge decks as they were designed for normal highway bridge loadings.

2 FEATURES OF BRIDGE25

Fig. 1 shows a photo of the completed Bridge25. This access bridge consistsof six 13.0m spans with five of the spans at 22.5m wide and the sixth span at 40.5m wide. The substructure of the bridge was founded on 800mm diameter Grade80 spun concrete piles driven to set at an average pile depth of approximately 36m. The piles

framed into reinforced concrete crossheads measuring 1.5m wide by 0.6m deep.

Structural analysis indicated that a total of 77 numbers of 1.4m deep by 1.6m wide conventional Grade50 precast concrete T-beams spaced at 2.0m centres will be required for the whole bridge deck. However, the T-beams came with a limitation of insufficient freeboard (i.e. 600mm) below the bridge soffit, therefore the beam depths had to be reduced. Hence, the UHPC option was considered in order to achieve the same high load carrying capacity required with a shallower beam depth, so that the minimum freeboard of 1m from the high tide water level can achieved. Fig. 2 gives a comparison of the cross sections of the composite bridge decks for both the UHPC and the conventional Grade50 concrete T-beam options. For the UHPC beam option, a total of 102 precast UHPC beams were required for Bridge25, with each UHPC beam spaced at 1.5m centre to centre. The UHPC beam option also gave a significant dead weight saving up to 66% per beam compared to the conventional Grade50 precast concrete beam design. The composite bridge deck was completed with a Grade50 in-situ RC deck, which has an average thickness of 300mm.

Fig. 1. Bridge25 using UHPC precast beams.

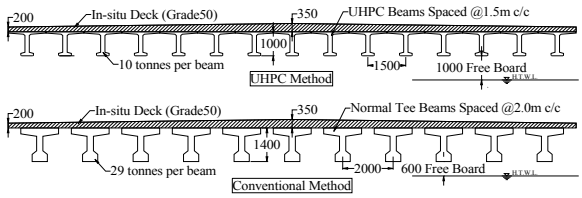

Fig. 2. Sectional views of Bridge25 deck options.

3 OVERSIZED CARGO LOAD

In Malaysia, bridges are mostly designed to the highway bridge traffic loadings specified in the Design Manual for Roads and Bridges (BD37/01). Bridge25 however, has to be designed for use by special trailers known as the "Goldholder 24 lines". According to the specialist transporter's specifications, these trailers are able to transport cargo payloads up to a maximum of 3,000 metric tonnes at a time. Factored live axle line loads of 387kN/axle and 458kN/axle for the serviceability limit state (SLS) and ultimate limit state (ULS), respectively were used in the structural analysis of the multi-span composite bridge.

4 GRADE150-UHPC

The raw materials for the Grade150 steel fiber reinforced UHPC used in the precast pretensioned beams include Type I ordinary Portland cement 42.5N; densified silica fume containing more than 92% SiO_2 with particle sizes ranging from 0.1μm to 1μm and surface fineness of 23,700m^2/kg and washed-sieved fine sand with particle sizes ranging between 100μm and 1,000μm. A polycarboxylic ether (PCE) based superplasticiser was used to ensure good workability of the mix. The micro steel fibers specified for the mix are required to have an ultimate tensile strength of 2,500MPa.

For this project, a bench mark value for performance was set for the UHPC material to achieve. It was specified that the average 28-day cube compressive strength and modulus of rupture shall not be less than 150MPa and 20MPa, respectively. Fig. 3 presents the statistical data on the various strength test results of the control specimens. Very strict quality control and inspection procedures were implemented during the production of the 104 prestressed precast UHPC beams for this project. (102 nos. for the bridge construction and 2 nos. for the destructive load test).

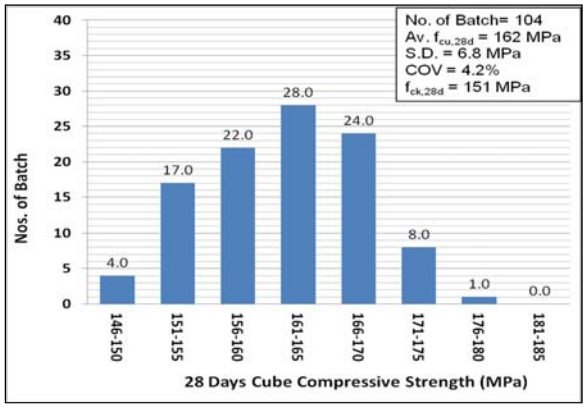

(a)

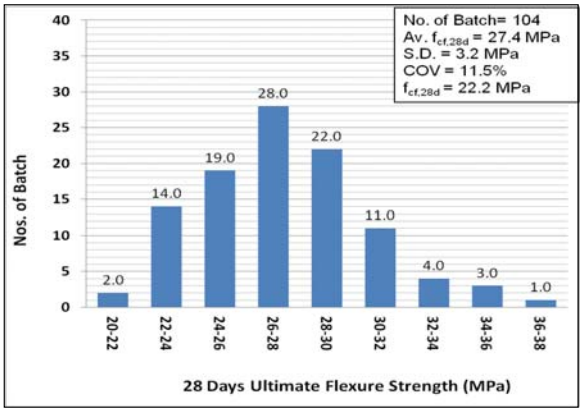

(b)

Fig. 3. Frequency distribution of 28-days (a) compressive strengths and (b) moduli of rupture for the UHPC material used in the precast beams.

Manufacturing of the first UHPC beam started in early April 2012 and completion of all 104 beams was not until the end of July 2012. Each single piece of precast beam was produced from a new batch mixing of the UHPC material, and control samples were collected from every batch of the UHPC mixes. For this project, a total of 104 sets of UHPC samples were collected (each set consisting of a minimum of six 100mm cubes and a minimum of one prism). Fig. 3 presents the statistical data on the various strength test results of the control specimens.

5 UHPC PRESTRESSED BEAM

Fig. 4 shows the cross-sectional dimensions of the UHPC beam used on Bridge25. The total length of the beam was 12.1m. The top flange was 1,490mm wide and reinforced with 6 pieces of 15.2mm diameter strands, while the bottom flange was 500mm wide and reinforced with 18 pieces of 15.2mm diameter strands. The web was designed as a thin membrane of 175mm in thickness.

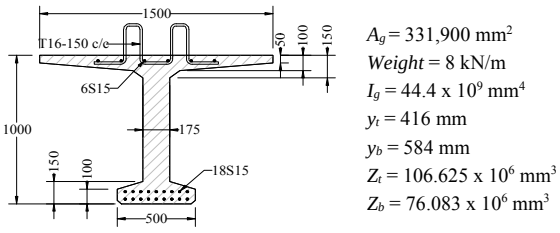

Fig. 4. Precast UHPC beam section details (in mm).

Unlike conventional RC beams where steel reinforcement or stirrups are used as primary resistance against all major tensile/shear forces that may occur in the stress/load path inside the beam; these UHPC beams do not have any conventional steel reinforcement or stirrups in its section other than the starter bars in the top flange. These starter bars are required only for making connection to the in-situ concrete deck. Instead, steel fibers are used to enhance the tensile-shear strength of the UHPC and to improve beam ductility.

6 SUSTAINABILITY DESIGN APPROACH (SDA)

Sustainability design approach (SDA) was used for the design of the above mentioned UHPC jetty. Fig. 5 presents the major three criteria for assessment of a sustainable design are:

(i) Environmental impact assessment (EIA),
(ii) Durability design (DD), and
(iii) Limit states design (LSD).

While there will be arguments as to the choice of an appropriate measure for sustainability, we shall adopt herein the environmental impact assessment (EIA). This criterion is a measure of the optimisation of the materials used with respect to the embodied energy and CO_2 emission when compared to existing practice. SDA suggests that durability design to be a sub-set of environmental impact design. Further, durability may be defined as the capability of a structure to meet its defined serviceability and strength limit state over time. Durability design is important to ensure the designed concrete structure meets the required design life, with as little maintenance as possible, thereby reducing the overall life-cycle cost, social impact and unplanned additional material consumption, which can bear heavily on future carbon impacts.

Finally, limit state design principles should be used to check for serviceability and strength requirements of the structure. If the aforementioned criteria can be adopted in any concrete structure design, the overall cost and functionality of a design structures can be optimised with minimum environmental impact.

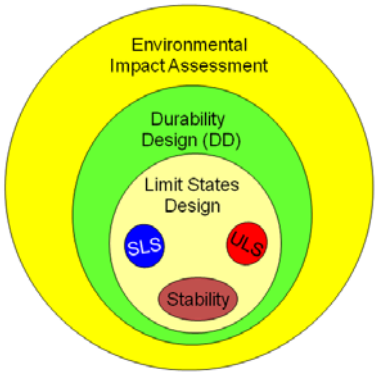

Fig. 5.Sustainability design approach (SDA).

6.1 ENVIRONMENTAL IMPACT ASSESSMENT (EIA)

This section firstly illustrates the example of EIA for Bridge25 based on the two different superstructure options shown in Fig. 2. The purpose of this exercise is to illustrate how the advancement of UHPC technology could help to reduce the carbon foot-print or to reduce the consumption of primary energy to construct the same bridge.

Table 1 summarises the inventory data of the materials used for this comparative study on the two bridges. Details on the derivation of this inventory data can be obtained from Voo and Foster (2010). The table has been prepared for determining the equivalent embodied energy (EE), CO_2 content and 100-year global warming potential (GWP) of each particular concrete mix design and the materials used. The information may be updated more frequently as the industry continues to improve its processes.

Elrod (1999) defines global warming potential (GWP) as a measure of how a given mass of greenhouse gas is estimated to contribute to global warming over a given time interval. It is a relative scale that compares the gas in question to that of the same mass of CO_2 and a 100-year of time horizon is most commonly adopted, as per the Kyoto Protocol (Forster et al. 2007). The formulation of GWP can be ambiguous and the adequacy of the GWP

concept has been widely debated since its introduction (Fuglestvedt et al. 2003). To-date, very little work has been done on this area and the relationship of 100-year GWP is yet to be unified. However, according to Voo & Foster (2010) and recommendation from FIB MC2010 Bulletin 66 (2012), the 100-year GWP can be written as:

$$100\text{-yr GWP} = CO_2 + 298\ NO_x + 25\ CH_4 \qquad (1)$$

In this comparative study, calculation of material quantities will only cover the superstructure, whereas the substructure is assumed to be the same for both cases. A comparison of the EIA results is presented in Fig. 6. In terms of material consumption, the UHPC option consumed 27% less raw material than the conventional option. In terms of environmental impact, the UHPC technology has 20.6% less embodied energy and 19% less CO_2 emissions. In terms of the 100-year GWP, the UHPC solution provides for a reduction of 14.5% over that of the conventional solution.

It also needs recognition that in this example only the savings at the level of the superstructure have been considered. Further savings will result from the lighter weight of the UHPC solution requiring a smaller substructure, foundations and lighter machinery and lower transport costs.

Table 1.– Inventory data for construction material (Voo and Foster, 2010).

	Cement Content	**Density**	**EE**	**CO_2**	**100-yr GWP**
Units	kg/m^3	kg/m^3	GJ/m^3	kg/m^3	kg CO_2 eq./m^3
UHPC$^{\uparrow}$	720	2,400	7.77	1,065	2,532
Grade50	480	2,350	2.70	480	978
Strands	-	7,840	185.8	17,123	34,392
Reo.	-	7,840	185.8	17,123	34,392

$\uparrow$ Environmental values include 2% by vol. steel fiber contribution

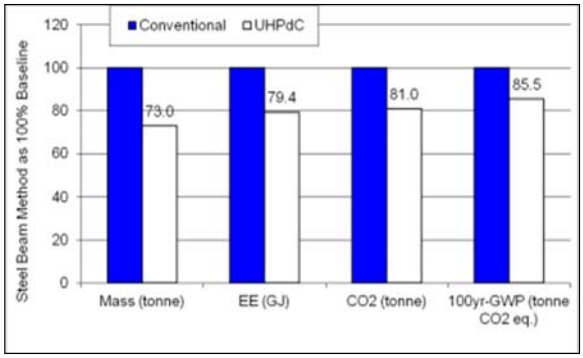

Fig. 6 – EIA comparison for Bridge25.

6.2 DURABILITY DESIGN

Throughout the world there are many RC structures suffering from corrosion, especially structures near coastal areas and in a marine environments. Many concrete bridges have been demolished due to heavy corrosion at ages of just 20 to 30 years and, in some cases, the maintenance costs far outweighed the initial construction costs (Yoshiki et al., 2001).

To-date, there is no one agreed unified method in the world to obtain a measure of the 'durability' of a concrete structure in aggressive marine conditions. However, the most commonly used or accepted model of service life prediction concerning the corrosion of the reinforcing bars was developed by Tuutti (1982).

Tuutti's model explains the service life of a concrete structure is composed of two periods, that is, firstly the initiation period (t_i) relative to the penetration of the chlorides or carbon dioxide (i.e., the aggressive agents, until the depassivation and the beginning of the corrosion of the bars) and; secondly the propagation period (t_p) where corrosion occurs. Such a criterion proposes the service life to be determined as a function of an acceptable limit of corrosion.

6.2.1 SERVICE LIFE

A certain group of researchers propose the criterion that the service life be defined as the initiation of corrosion ONLY. The justification of this criterion is that once the corrosion has begun, the full process develops fast, especially in the case of attack by chlorides. The reason for such contention is that the second stage (i.e. the propagation period, t_p) is an extremely complex subject due to a structure can has vast distinguished level of exposures, such as level of chlorides ingression, relative temperature and humidity, freeze and thaw attack, concrete grades, quality control during placing or manufacturing and many others to just list a few. Therefore in this paper, the service life of a structure is considered as the initiation period only as shown in Eq. 2.

$$Service\ Life = t_i \qquad (2)$$

The concept of chloride attack due to chloride ions permeating into reinforced concrete are illustrated in Fig. 7. The matrix of normal concrete is analogous to that of a sponge where the air voids, micro-pores, gel-pores and capillaries are inter-connected to each another. These micro-pores and gel water, which are generally formed in the concrete matrix, serve as routes for the movement of chloride ions or other aggressive elements. The pore structure in concrete depends on the type of concrete, mix proportion, type of formwork, placing technique, curing method, heat of hydration and material quality, W/C ratio, presence of additive and others. Near coastal areas, where high levels of air-borne chlorides exist, and where parts of structures lie in the splash zone, large quantities of chloride ions can adhere to the surface. The chloride ions then permeate and reach the concrete surrounding steel reinforcement. Chloride ions can break the passive oxide film and initiate corrosion even under highly alkaline condition. Thus, typical heavy cracking and spalling of concrete due to corrosion expansion of reinforcing steel may take place early.

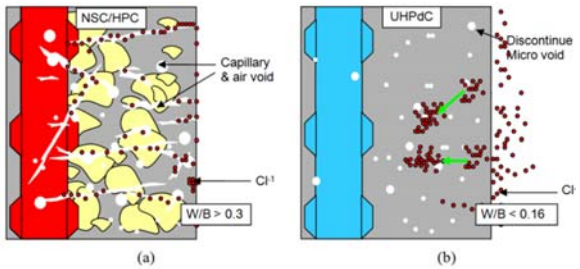

Fig. 7 - Comparison of concrete matrix of (a) ordinary concrete against (b) concrete matrix of UHPC.

UHPC has a densely packed microstructure (refer to Fig. 7b) in which the W/B ratio is lowered to below the hydration limit (typical W/B ratio of UHPC is 0.16 or less). Thus air voids are significantly reduced and are discontinuous in the matrix. The chloride diffusion coefficient (D_c) of UHPC is at least one to two order less than normal concrete. Therefore in the presence of chloride ions at the surface of the concrete, the amount of time needed for the chloride ions to diffuse through the UHPC concrete cover and initiate depassivation of the steel increases dramatically. Of course, this assumption is only valid provided the concrete is uncracked.

In this comparative study, the concrete cover used in Grade 50 HPC beam and Grade150 UHPC girders are taken as 50mm and 22mm, respectively. Both the bridge girders are exposed to airborne chloride ion attack. The durability prediction is governed by Fick's 2nd law of diffusion (Andrade, 1999; FIB Model Code, 2012), that is Eq. 3:

$$C_X = C_S\left[1 - erf\left(\frac{X}{2\sqrt{D_c\, t_i}}\right)\right] \qquad (3)$$

where X is the distance of the outermost steel reinforcement from the concrete surface (in mm) also known as the concrete cover, t_i is the time (in seconds), D_c the chloride diffusion coefficient constant (in mm^2/sec.), *erf* the error function, C_s the chloride ion concentration at the surface of the uncracked concrete and C_x is the critical chloride threshold concentration for steel corrosion.

6.2.2 Surface Chloride Concentration (C_s)

The C_s value used in this example is the airborne chloride concentration based on the work by Yoshiki et al. (2001). The airborne chloride concentration $C_{s,airborne}$ (in kg/m^3) can be calculated from Eq .4 where D is the distance (in km) from the coast. Assuming the two bridges are located 1m from the coast, then using Eq.4, the value of C_s = 6.4 kg/m^3 is obtained. For structures submerge in the sea water, the C_s value can be taken as $C_{s,submerge}$ = 19.3 kg/m^3 for the ocean or sea with a salinity of 3.5%.

$$C_{s,airborne} = \frac{1.22}{D^{0.24}} \quad where \quad 1m \le D \le 10km \qquad (4)$$

$$C_{s,submerge} = 19.3 \quad \text{for sea with 3.5\% salinity}$$

6.2.3 Chloride Threshold Concentration (C_x)

The chloride threshold concentration in concrete is most commonly expressed as *total chloride content relative to cement weight*. Its defines as the limit of total chloride present at the steel reinforcement level where corrosion initiated due to depassivation of the reinforcement has taken place. A lot of studies have been undertaken in order to find chloride threshold values in cement based materials and the reported results scatter over several orders of magnitude (Angst & Vennesland, 2009). This large span of results might be due to several reasons: First, different definitions for critical chloride content have been used; second, various techniques to find critical chloride contents have been applied by different researchers and, last but not least, critical chloride content is a complex matter that depends on a variety of influencing factors. Major parameters are the pH of the pore solution, the electrochemical potential of the steel and the quality of the steel-concrete interface.

Table 2 shows the critical chloride threshold concentration value can range from 0.2% to 0.35% by weight of the cement content in the concrete mix. For comparison purpose, this paper adopted a value of C_x = 0.3% as per recommendation from BA35/90 (1990) for the chloride threshold value.

Table 2. Chloride threshold at different concrete grade.

Source	C_x (% by wt. of cement)	C_x Values (in kg/m^3) NSC G40	HPC G60	UHPC G150
Cement Content	-	350	480	720
BA 35/90 (1990)	**0.30**	**1.05**	**1.44**	**2.16**
BS8110:Part1 (1997)	0.35	1.23	1.68	2.52
Paul et al. (2005)	0.20	0.7	0.96	1.44

6.2.4 Chloride Diffusion Coefficient Constant (D_c)

Chloride diffusion is implicitly considered through the specification of W/C ratio, cementitious materials content and type, and in the compaction and curing requirements. These implicit considerations, however, do not provide control to the property, but rather a range of likely values for the material. To-date, there is no one agreed method to obtain this diffusion value based on above mentioned specification. Having said that, the Ash Development Association of Australia (ADAA, 2009) has published a simple empirical correlation of the chloride diffusion constant versus concrete strength (see Fig. 8). Using this empirical relationship, the Grade 50 concrete can be assumed to have a D_c value of 3.0 x 10^{-6} mm^2/s. For the UHPC beam, the D_c value was measured experimentally by Voo & Foster (2010) and it is taken as $D_{c,UHPC}$ = 6.87 x 10^{-8} mm^2/s.

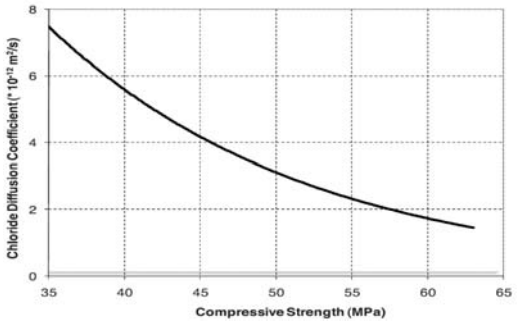

Fig. 8 - Typical data for chloride diffusion coefficient versus fly ash concrete compressive strength (Note: fly ash contents range between 25% to 35% by mass of binder). (Source: ADAA, 2009).

6.2.5 2nd Fick's Law of Diffusion

Eq.3 is the simplest and mostly widely accepted equation that expresses the process of chloride ingress from outside with the minimum required parameters. The results in Table 3 show that with a concrete cover of 50mm, and without intervention or any active corrosion prevention systems, corrosion of the reinforcing steel in the Grade50 concrete beams will initiate after just 10.5 years. In contrast, depassivation in the UHPC beam will not start for 154 years. Thus without regular maintenance, or passive or active corrosion protection systems, many conventional concrete structures in marine environments fail at an early age. In comparison UHPC structures have the potential for significant savings in maintenance costs and a longer service life, leading to sustainable solutions. This is particularly true if the structural element is pre-compressed to avoid cracking under service conditions.

Table 3 – Durability calculation in marine environment.

Exposure	**Air-borne salt**	
Concrete Type	Grade50	UHPC
Cement (kg/m^3)	480	720
f_{ck} (MPa)	50	150
X (mm)	50	22
C_s (kg/m^3)	6.403	6.403
C_x (kg/m^3)	1.68	2.52
D_c (mm^2/s)	3.0 x 10^{-6}	6.87 x 10^{-8}
Time (years), t_i	10.5	153.5

7 LIMIT STATE DESIGN

Bridge25 was designed as a six-span continuous composite bridge with rigid joints at the supports. Table 4 summarises the critical design force effects both in terms of SLS and ULS from the structural analysis of Bridge25. The design bending moment and shear force resistances for both the precast beam and the composite bridge can be computed from the provision of JSCE (2006).

Table 4 – Design force effects.

	Design Forces	**Positive Moment kNm**	**Negative Moment (kNm)**	**Shear Force (kN)**
Composite Bridge	SLS	2,156	-2,282	1,299
	ULS	2,558	-2,709	1,541
	Resistance	4973	-3274	1866
Precast Beam Only	SLS	1,517	-	1,024
	ULS	1,895	-	1,218
	Resistance	3750	-	1420

8 DESTRUCTIVE PERFORMANCE LAOD TEST

Prior to the construction of Bridge25 and to verify the strength of the precast UHPC beam's strength, the Client and the Engineer had requested for full scale performance load tests on the UHPC beams both in flexure and in shear until failure. For the purpose of the verification load tests, only the precast beams (i.e. without the RC deck) were tested. First principles of solid mechanics were used to calculate the design load actions on the beams in the absence of the deck. The calculations show that the precast UHPC beam only (without the deck) will resist 74% of the design bending moment effect and 79% of the design shear force effect of the composite section. These values are tabulated in Table 4. The UHPC beam manufacturer had guaranteed that the precast UHPC beam only (without the deck) would be able to resist a minimum design moment of $M_{Rd,beam}$= 3,750kNm and a minimum design shear force of $V_{Rd,beam}$= 1,420kN. Two prototype UHPC beams were forthwith manufactured and subjected to the strength verification tests as described below.

8.1 Flexural Strength Test

The detail set up for the flexural strength verification test can be obtained in Ikram (2011). The test was conducted at the heavy structural laboratory of Dura Technology Sdn Bhd. Fig. 9 shows the flexural beam was set in a three point test configuration with a simply supported span of 11.9m. The applied force from the hydraulic jack was placed at the centre of the span with a stiff steel plate/beam to distribute the load across the top flange of the beam. One end of the beam was supported on a pinned support, while the other end was sitting on a pin and roller support. The pins and rollers were greased to minimise friction in order to give the required freedom of rotation and horizontal translation.

Three sets of Linear Variable Differential Transformers (LVDTs) were used to capture the vertical displacements of the beam during testing. LVDT1 was the major interest of the test as it was located at the midspan of the beam (i.e. where the applied load was situated). LVDT2 and LVDT3 were placed at both supports to monitor support stiffness. The results of flexural tests are presented in Fig. 9, where $P_{cr,exp}$ denotes the applied load measured at first structural cracking, determined by visual tracing of cracks on the specimens or as detected on the load versus displacement curves (whichever was lower),

and the symbol $P_{u,exp}$ denotes the maximum applied load recorded at the end of each test.

As the cracks were extremely fine and difficult for the naked eyes to trace, water was sprayed onto the surface of the beam at each load step, to help obtain a clearer trace of the cracks. In the flexural strength test, the first flexural cracks were observed at the applied load of $P_{cr,exp}$= 870kN. Using a microscopic crack detector, the crack widths observed were in the order of 0.01mm under this load. The cracking moment capacity (M_{cr}) of the beam can therefore be calculated as follows:

M_{cr} = Applied load x Span/4 + moment due to SW of girder = 870 x 11.9/4 + 8 x 11.9^2/8 = 2,730 kNm.

The resulting M_{cr} proved that the UHPC beam did not crack at the Design SLS load condition (see Table 4). As the applied load increased further through the test, more cracks were formed but the cracks were fine and uniformly distributed across the span. Observations show that these multiple flexural micro-cracks, which appear "smeared" across the bottom flange/web area, have crack widths of approximately 0.2mm to 0.3mm at the applied load of P = 1,230kN, corresponding to the guaranteed load carrying capacity in flexure ($M_{Rd,beam}$). As a result, the Design ULS load condition was met.

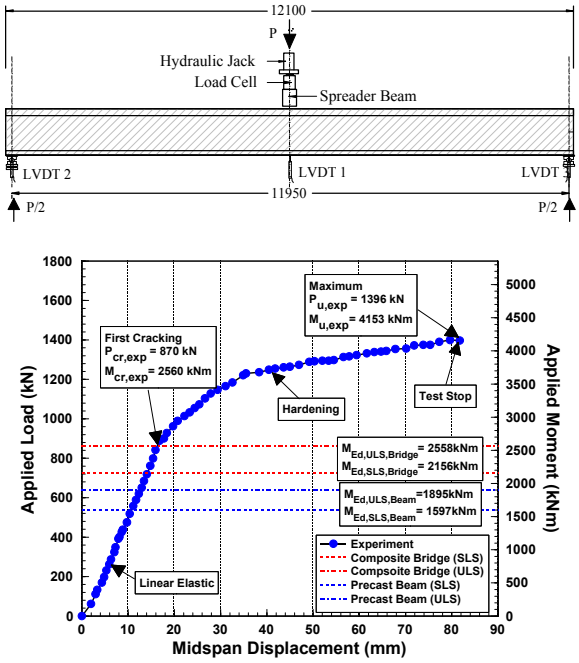

Fig. 9 – Flexural test setup and experimental result compared against design moments criteria.

The maximum applied load captured in the flexural test was P = 1,396kN, which corresponded to a maximum applied moment of 4,153kNm at the midspan, confirming that the UHPC beam had ample positive moment resistance over the design positive moments shown in Table 4. The resulting plot of the applied load versus midspan displacement curve of the test beam in Fig. 9 also show that the test beam exhibited linear elastic behaviour prior to cracking. The midspan deflection at first cracking was captured to be 16mm. The beam was able to undergo a further 64mm of midspan deflection before the maximum applied load of P_u = 1,396kN was reached.

8.2 Shear Strength Test

The detailed set up for the shear strength verification test can be obtained in Ikram (2011). Fig. 10 shows the shear beam was simply supported over a span of 5.67m between centrelines of the supports. The applied concentrated load was similarly placed at the top flange of the beam in a three point test configuration. The ratio of shear span to effective depth used in the shear test was 2.

In the shear strength test, the measured first cracking load was P_{cr} = 2,130kN (i.e. V_{cr}=1,420kN) which co-incidentally equalled the guaranteed shear force capacity of the UHPC beams ($V_{Rd,beam}$). Assuming that the shear force was taken by only the rectangular section of the web, the cracking shear strength of the beam can be approximated as, τ_{cr} = 2130 x 2/3/(175 x1000) = 8.1MPa.

Fig. 10 shows the plot of the applied load versus displacement curve of the beam tested in shear. Beam deflection generally showed linear elastic behaviour before cracking. The monolithic section underneath the applied load (i.e. near LVDT1) was captured with a deflection of 8mm at the first web shear cracking load effect of V_{cr} = 1,420kN. After first shear cracking, the beam exhibited displacement hardening behaviour until the maximum applied load of P_u = 2,761kN (V_u = 1,841kN) was recorded. The shear test clearly demonstrated that the UHPC beam section had sufficient reserves in shear resistance beyond the design shear force (see Table 4).

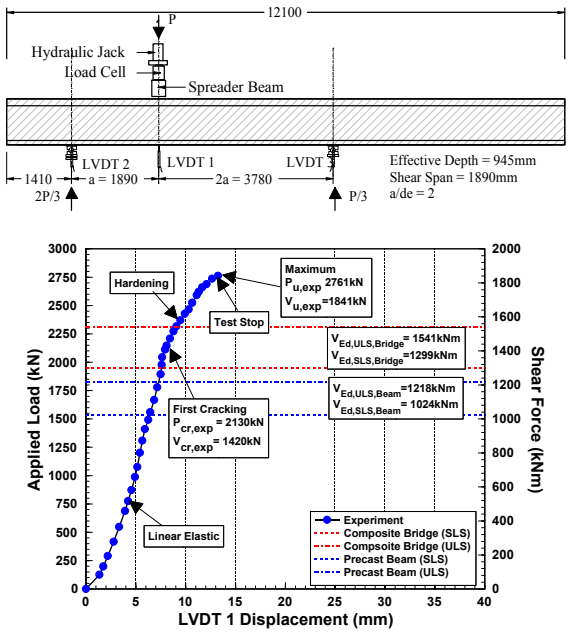

Fig. 10 – Shear test setup and experimental result compared against design shear forces criteria.

9 CONCLUSION

The Bridge25 project provided a unique set of challenges which afforded the Engineer an opportunity to explore the use of UHPC technology in the design of the multiple span composite bridge for the marine environment.

In the process of design the Engineer gained valuable exposure to the properties of the material, which imparts unique mechanical behaviour to the beams made from it. These include the high strength obtained from a 1m deep section, the generous reserve capacity after cracking and the ductility that were seen in the test results.

The various and multiple tests gave confidence to the Engineer with regard to the ability of the UHPC beams to fulfil their roles. Such confidence can only be the result of the meticulous selection of materials and careful control of the manufacturing processes. Bridge25 provided a live platform to compare and contrast the performance of UHPC against conventional concrete in terms of strength, durability, material consumption, embodied energy, CO_2 content, embodied energy and global warming potential. The experience with UHPC has certainly left the Engineer in a much better position to tackle the questions of durability and sustainability.

REFERENCES

ADAA., 2009. "Fly Ash Concrete in Marine Environments", *Fly Ash Technical Note No.4*, Ash Development Association of Australia, Nov., pp: 1-3.

Andrade, C., 1999. "Chloride Penetration Model", *International Specialist Workshop – Design of Durability of Concrete*, Berlin, 15-16th June.

Angst, U., and Vennesland, Ø., 2009. " Critical Chloride Content in Reinforced Concrete – State of the Art", *Concrete Repair, Rehabilitation and Retrofitting II – Alexander et al. (eds),* pp: 311 - 317.

BA 35/90, 1990. Inspection and Repair of Concrete Highway Structures, Vol.3, Section 3.

BD37/01, 2001. "Loads for Highway Bridges", *Design Manual for Road and Bridge*, Volume 1, Section 3, Part 14, 106pp.

BS8110: Part 1, 1997. "Structural use of concrete. Code of practice for design and construction", *British Standard,* British Standards Institution, ISBN:9780580598937.

Elrod, M., 1999. "Greenhouse Warming Potential Model", *Journal of Chemical Education*, Vol. 76, No. 12, pp: 1702-1705.

Forster, P., et al., 2007. Changes in Atmospheric Constituents and in Radiative Forcing. In: S. Solomon et al. eds. Climate Change 2007: The Physical Science Basis. Contribution of Working Group I to the Fourth Assessment Report of the Intergovernmental Panel on Climate Change. Cambridge. United Kingdom and New York, NY, USA: Cambridge University Press.

Freytag, B. et al., 2012. "WILD-Bridge Scientific Preparation for Smooth Realisation," *Proceedings of Hipermat 2012 3rd Int. Symposium on UHPC and Nanotechnology for High Performance Construction Materials*, Ed., Schmidt, M., Fehling, E., Glotzbach, C., Fröhlich, S., and Piotrowski, S., Kassel University Press, Kassel, Germany, pp: 881–888.

Fuglestvedt, J.S. et al., 2003. "Metrics of Climate Change: Assessing Radiative Forcing and Emission Indices", *Climate Change*, 58, pp: 267–331.

Ikram, 2011. "Flexure and Shear Strength Test of T-Bridge Girder (TBG1325)", *Test Report FS6A01/454/11*, Material Testing Laboratory Ikam QA Service Sdn Bhd, 20 pp.

JSCE, 2006. "Recommendations for Design and Construction of Ultra High Strength Fiber Reinforced Concrete Structures (Draft)", September, Concrete Committee of Japan Society of Civil Engineers (JSCE), *JSCE Guidelines for Concrete No. 9*, ISBN: 4-8106-0557-4, 106 pp.

MC2010, 2012. Model Code 2010 – Final Draft. Bulletin 66. CEB-FIB. Volume 2., 370 pp.

Paul, J.T., David, P. and Pavel, M., 2005. "Statistical Variations in Chloride Diffusion in Concrete Bridges", ACI Structural Journal. May-June, pp: 481-486.

Tuutti, K., 1982. "Corrosion of Steel in Concrete", *Swedish Cement and Concrete Research Institute*, Nº F04, Stockholm, 469 pp.

Voo, Y.L. & Foster, S.J., 2010. "Characteristics of Ultra-High Performance 'Ductile' Concrete (UHPdC) and its Impact on Sustainable Construction", *The IES Journal Part A: Civil & Structural Engineering,* Institute of Engineering Singapore, Vol. 3, No. 3, August, pp: 168-187.

Yoshiki, T., et al., 2001. "Study on Required Cover Depth of Concrete Highway Bridges in Coastal Environment", *17th US-Japan Bridge Engineering Workshops*, Tsukuba, pp: 1-16.